

# TOWARDS FULL PERFORMANCE OPERATION OF SwissFEL

T. Schietinger\* on behalf of the SwissFEL team  
 Paul Scherrer Institut, CH-5232 Villigen, Switzerland

## Abstract

SwissFEL is the new X-ray free-electron laser facility at the Paul Scherrer Institute (PSI) in Switzerland. It was inaugurated in December 2016 and saw its first pilot experiments at the end of 2017. We describe the commissioning steps leading to the first phase of pilot experiments and outline the plans towards reaching nominal performance levels in 2018.

## INTRODUCTION

The newest large research facility at the Paul Scherrer Institute, the hard-X-ray free-electron laser SwissFEL [1] has recently commenced its scientific program with a series of pilot experiments. SwissFEL aims at delivering ultra-short coherent photon pulses through two beam lines called Aramis (hard X-rays, 1–7 Å) and Athos (soft X-rays, 6.5–50 Å). So far only the Aramis beam line has been commissioned with two experimental stations in operation, called Alvra and Bernina. Alvra is a multipurpose pump-probe station focusing on ultrafast biology and chemistry, while Bernina specializes in pump-probe crystallography for the study of ultrafast dynamics in solid matter, in particular strongly correlated systems, as well as structural biology. A third endstation, Cristallina, will be realized at a later stage. Its primary focus will be coherent diffraction imaging.

The SwissFEL accelerator consists of an electron source, an S-band (3 GHz) booster linac and a C-band (5.7 GHz) main linac (Fig. 1). The electron source is a laser driven 2.5-cells S-band RF photoinjector gun. The electron bunches, with charge ranging between 10 and 200 pC, are longitudinally compressed in two stages at nominal energies of 320 MeV and 2.1 GeV, respectively. A higher-harmonic cavity (X-band, 12 GHz) linearizes the electron phase space before the first compression stage.

The accelerated and compressed electron bunches are sent into the Aramis undulator line comprising 13 in-vacuum undulator modules of 4 m length each. A second undulator line, Athos, is currently under construction. It will be driven by 3 GeV electrons extracted in a switchyard halfway along the main linac. Table 1 lists the most important parameters of the SwissFEL facility.

## FIRST LASINGS

The commissioning of the SwissFEL facility is largely driven by the availability of the RF stations and the consequently accessible beam energy. The earliest attempt at lasing in the undulator line was made at the occasion of the official inauguration of the facility in December 2016, with only two S-band RF stations in the injector and one C-band

station in the first linac, resulting in a total beam energy of 380 MeV. With this beam energy, the first FEL radiation with an estimated photon energy of 50 eV could be observed with a photodiode installed in the front end. By May 2017 enough RF stations had been commissioned to attempt lasing in the (soft) X-ray regime. Using the full injector energy of 300 MeV and three C-band stations in linac-1, a total beam energy of 910 MeV was reached, resulting in lasing at a photon wavelength of 4.1 nm (300 eV photon energy) [2]. The declared project goal for 2017 was to have first pilot experiments in the two experimental stations before the end of the year. To reach this goal, it was essential to have a short period of photon delivery at a minimum energy close to 1 keV to allow for the commissioning of the most important optics components leading to the experimental halls. With six C-band stations available in August 2017, lasing was established at an electron energy of 1.62 GeV, delivering photons of 1.28 nm wavelength (970 eV) to the optics hutch. The electron energy was then further increased to 2.45 GeV by November 2017, allowing the first SwissFEL pilot experiment to be performed at a photon energy of 2.2 keV. A second pilot experiment followed only two weeks later with somewhat higher energies. Table 2 summarizes the first lasings achieved by SwissFEL. Up to now, the repetition rate has been set to 10 Hz during all lasing periods. In Fig. 2 we give a schematic overview of the achieved lasing performance as well as our plans to reach the nominal performance level of SwissFEL, i.e., 12.4 keV photon pulses (generated with a 5.8 GeV electron beam) at a repetition rate of 100 Hz.

## PILOT EXPERIMENTS

Four pilot experiments have been carried out at SwissFEL so far. In the very first, performed in November 2017 at the Bernina experimental station, Ti<sub>3</sub>O<sub>5</sub> nanocrystal samples were excited (“pumped”) with infrared laser light (800 nm, 42 mJ/cm<sup>2</sup>) and probed by the 3rd harmonic photons (6.6 keV) of the FEL radiation (fundamental at 2.2 keV). The goal of the experiment was a time-resolved study of the dynamics of the semiconductor-to-metal transition in this material, which has potential applications in data storage.

Table 1: SwissFEL Main Parameters

Parameter	Value
Photon wavelength	0.1–5.0 nm
Photon energy	0.25–12.4 keV
Pulse duration	1–30 fs
Electron energy	5.8 GeV
Electron bunch charge	10–200 pC
Repetition rate	100 Hz

\* thomas.schietinger@psi.ch

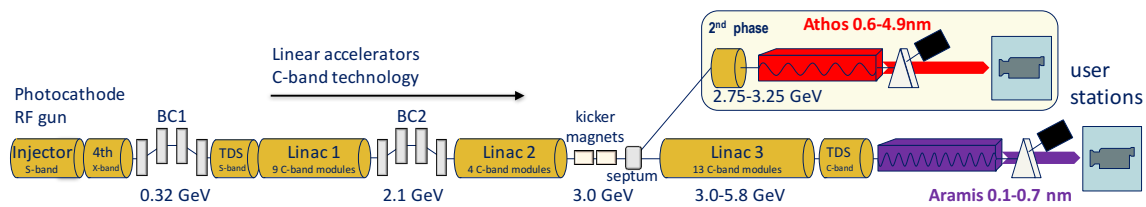


Figure 1: Schematic of SwissFEL accelerator layout (from Ref. [1]).

Table 2: First Lasings at SwissFEL

Date	Purpose	Electron energy	Photon energy (wavelength)	Photon pulse energy	Rep. rate
Dec. 2016	Inauguration	380 MeV	24 nm (50 eV)	not measured	10 Hz
May 2017	IPAC'17	910 MeV	4.1 nm (300 eV)	30 $\mu$ J	10 Hz
Aug. 2017	First photonics commissioning	1.62 GeV	1.28 nm (970 eV)	9.5 $\mu$ J	10 Hz
Nov. 2017	First pilot experiment (Bernina)	2.45 GeV	0.55 nm (2.2 keV)	220 $\mu$ J	10 Hz
Dec. 2017	Second pilot experiment (Alvra)	2.6 GeV	0.54 nm (2.3 keV)	250 $\mu$ J	10 Hz

The second pilot experiment, which was the first to be carried out at the Alvra experimental station, was dedicated to the investigation of UV photo-induced charge transfer in an OLED candidate material based on copper and phosphorus. To characterize the role of the phosphorus atoms in the charge transfer, X-ray emission spectroscopy was applied with an incoming photon energy of 2.34 keV.

In March 2018 two further pilot experiments were performed, studying ultrafast lesion formation in DNA (Alvra, with 2.15 keV photons) and THz switching of ferroelectric polarization in  $\text{Sn}_2\text{P}_2\text{S}_6$  (Bernina, 2.0 keV). As part of the Bernina experiment the Bragg intensity changes from optically pumped phonons were measured for the Bi(111) benchmark system. From the observed modulation the time resolution of the experimental setup, still before pulse-to-pulse timing corrections, was estimated to be about 110 fs (rms) (see Fig 3).

## STATUS AND PLANS OF KEY SYSTEMS

In the following we briefly describe the status of some key systems crucial for the FEL performance and our plans to ensure attaining the nominal performance level by the end of this year.

### Electron Source

The RF gun, designed and manufactured at PSI, was thoroughly tested at the SwissFEL Injector Test Facility [3]. Since its recommissioning at SwissFEL it has produced electron bunches of 7.1 MeV with excellent stability and reliability. A spare gun is in production to ensure redundancy for the coming years of user operation.

The electrons are extracted by a UV laser from a  $\text{Cs}_2\text{Te}$  coated copper photocathode installed in the backplane of the gun. At present SwissFEL is operating with its second photocathode: in July 2017 the originally installed photocathode was replaced by the current one, which has a somewhat lower quantum efficiency, but features a uniform distribution around the area illuminated by the laser without any signs of deterioration during its time of operation. The measured quantum efficiency is on the order of 1%, largely sufficient to generate the SwissFEL nominal bunch charge of 200 pC.

The primary gun laser system is based on a solid-state  $\text{Yb:CaF}_2$  chirped amplifier providing excellent stability and uptime. The laser spot size on the cathode is controlled through a series of apertures constraining the laser beam propagated to the gun. In the longitudinal dimension, a flat-top profile is approximated through pulse-stacking. The profile can be optimized beam based by directly observing the electron bunch profile with an RF deflecting cavity or simply by maximizing the resulting FEL power.

A backup laser system (Nd:YLF) yielding a fixed Gaussian longitudinal profile is available and used for comparison studies. Once the timing is set up for both laser systems, the switching between the two is instantaneous, which has

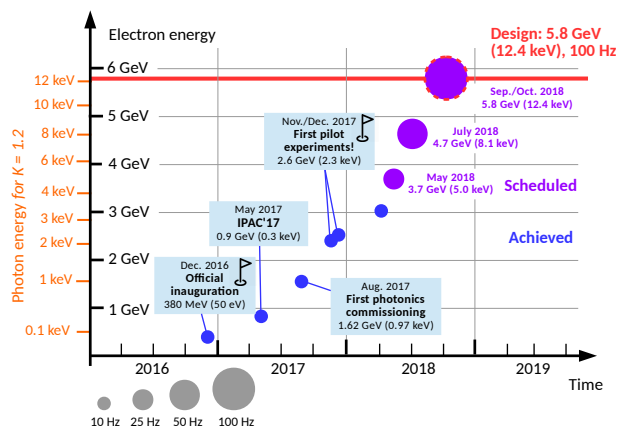


Figure 2: Schematic illustration of SwissFEL performance evolution, with future progress scheduled for 2018.

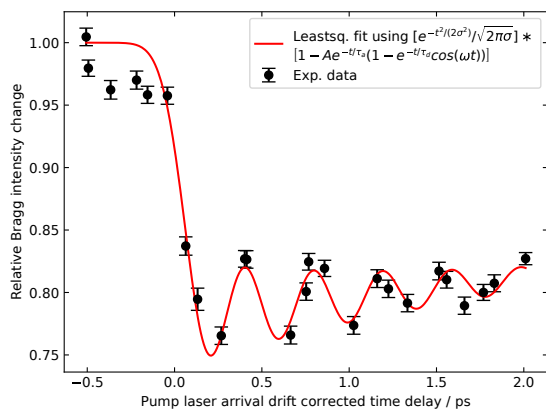


Figure 3: Relative Bragg intensity measured on Bi(111) film as a function of pump-probe delay time, showing the characteristic modulation from optically pumped phonons.

proven very valuable during the commissioning of the accelerator. Since this second laser does not provide the full functionality of the primary laser, it is planned to procure a true identical backup system for complete redundancy.

The merits and drawbacks of different longitudinal laser profiles are the subject of ongoing studies. It is foreseen to modify the primary laser system in such a way that it can provide a stretched (truncated) Gaussian pulse of variable length, thus adding more freedom to the optimization process.

The stable and highly reproducible performance of the entire gun-cathode-laser system is an important precondition for the successful setup of the FEL. We therefore developed a standard operating procedure that ensures a systematic setup of this complex including the verification and documentation of the most important characteristics of the system. The procedure is systematically applied at every restart of the accelerator, occasionally also during operation periods in case of doubts or suspicions.

Recently performed tests generating electrons at 100 Hz have been successful, therefore no immediate problems are expected from that system when permanently increasing the repetition rate to its nominal value.

Further development steps include the stabilization of the UV laser arrival time by means of an arrival-time monitor and the setup of dual-pulse generation for the simultaneous operation of the Aramis and Athos beam lines.

### C-Band Linac

The C-band main linac [4] is the centerpiece of the Swiss-FEL accelerator defining the available electron and hence photon energy. It consists of a total of 26 RF modules, each providing a nominal accelerating voltage of 240 MV with four tuning-free copper structures. The effectively achieved accelerating voltages vary between 200 and 280 MV, depending on the conditioning states of the modules. In each station, an IGBT-switched solid-state modulator manufactured by

Ampegon (first half of the linac) or ScandiNova (second half) drives an E37212 Toshiba klystron, which can furnish up to 50 MW for a duration of 3  $\mu$ s. The RF pulse is compressed in a barrel-open-cavity (BOC) before being delivered to the four structures via a precisely adjusted waveguide network.

Currently 13 of the 26 stations are available for beam acceleration. In the present configuration, the linac delivers 2.7 GeV for a total energy of 3.0 GeV (300 MeV from the booster), with about 0.5 GeV of reserve to maintain a constant energy for the experiments also after a module failure.

The commissioning of the remaining modules is on track for raising the beam energy towards the nominal 5.8 GeV by the end of the year. In the current schedule, the operational beam energy is slated to be increased to 3.7 GeV by mid May using a total of 16 C-band modules and further to 4.7 GeV (with 22 modules) by mid July. In this schedule, the final beam energy will be reached by mid September making use of 24 C-band modules. At every stage the schedule provides ample reserves to maintain the beam energy at least for the case one single module fails.

All C-band modules are systematically operated at 100 Hz, even if electron bunches only come along at 10 Hz. Recent tests with a low-charge beam at 25, 50 and 100 Hz basically demonstrated beam transport at these rates, but a detailed assessment of associated stability issues is still pending. The overall objective is to run the facility with a beam energy of 5.8 GeV at a repetition rate of 100 Hz by September of this year.

### Aramis Undulator Line

The basic commissioning and electron-beam-based alignment of the undulator line, using the corrector-based method described in [5], has been done. In parallel a photon-based method for the fine-tuning of the undulator parameters [6] has been implemented and tested successfully. In a next step the procedures will be refined to allow for a systematic comparison between their results. The goal is the establishment of a swift but accurate beam-based alignment procedure to be applied during the preparation of every run period.

### Electron Beam Diagnostics

During user operation the electron beam position is stabilized in the transverse directions through an orbit feedback, which uses the displacements measured by resonant-cavity beam-position monitors (BPMs) [7]. At three locations along the machine (magnetic compression and energy collimator chicanes) BPM signals in dispersive sections are used to run energy feedbacks.

Furthermore the bunch length after the first compression stage is stabilized by keeping constant the signal of a dedicated compression monitor measuring the radiation emitted by the compressed bunch at the edge of the last dipole of the chicane, which in this case falls in the THz spectral range [8]. The optimal compression signal to lock on to is found through pulse-to-pulse correlation with the FEL output signal (delivered by a photon gas detector). Another compression monitor located after the second compression

Content from this work may be used under the terms of the CC BY 3.0 licence (© 2018). Any distribution of this work must maintain attribution to the author(s), title of the work, publisher, and DOI.

stage is currently being commissioned and will soon become available for experiment runs.

Additional longitudinal stabilization will be provided by a series of high-resolution bunch-arrival-time monitors, currently also under commissioning [9]. Initial commissioning work on the first of these monitors, installed after the first compression stage, yielded a resolution of about 5 fs and a preliminary value for the arrival-time jitter at this position of 35 fs. This value is expected to improve considerably after the recent installation of a new preamplifier for the X-band RF module, whose phase is known to be one of the most critical parameters affecting the beam arrival time.

For the setup and verification of beam optics and compression, the primary diagnostics consists in insertable scintillating screens (YAG crystals) [10]. The commissioning of wire scanners, to be used for the semi-invasive measurement of transverse beam sizes, is still ongoing.

## BEAM DYNAMICS PROGRESS

### Optics and Emittance

After some initial difficulties related to usual startup commissioning troubles the beam optics is now well understood throughout the machine. The systematic optimization of the beam emittance at the source has brought about projected emittances of less than 250 nm and slice emittances of around 150 nm for the standard bunch charge of 200 pC within 10 ps (FWHM) (uncompressed beam). Figure 4 shows the initial emittance optimization performed in July 2017, in which the projected emittance is measured for various combinations of laser spot size on the cathode and gun solenoid focusing strength.

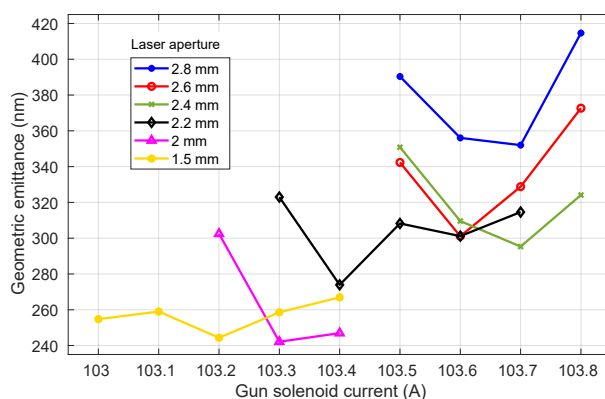


Figure 4: Emittance optimization at the electron source.

### Compression Setup

In the first compression stage, the electron bunches are systematically compressed by use of two compression “knobs” constructed from the amplitude and phase settings of the relevant S- and X-band RF stations [11]. The established compression procedure allows setting bunch lengths down to 120 fs (rms), with only minor increase in slice emittance, as verified with the S-band RF deflector.

Since the C-band deflector following the second compression stage was only commissioned in January 2018, the compression in the second stage was set up empirically (or not used at all) for the first lasings. Systematic studies towards an optimal dual-stage compression setup using the RF deflector are still ongoing. For the last experiment runs the bunch length was compressed down to about 50 fs (rms).

### Laser Heater Setup

The laser heater system [12], designed and built in collaboration with ASTeC to suppress the microbunch instability, has undergone only preliminary commissioning. The overlap between the laser and the electron beam has been achieved both transversally and longitudinally, and the characteristic increase in energy spread has been observed, both for projected and core beam. A more thorough commissioning as well as detailed characterization measurements are still needed before the system can be applied for routine operation.

## FEL SETUP AND CHARACTERIZATION

Once the beam optics is set and verified and the beam is compressed to have an appropriate peak current, our current FEL setup procedure entails the following steps: first, a gain curve is measured by successively closing the gaps of the undulator modules along the beam line while measuring the photon pulse energy with a gas detector installed in the front end. Based on this gain curve, the optimal pre-saturation taper profile (linear, to compensate for energy loss due to wakefields in the undulators) is found and set. Then, the individual  $K$  values and phase shifter settings are adjusted, if necessary, to ensure uniform gain in all undulator modules. The next step consists in the optimization of the post-saturation taper profile (linear and quadratic, to compensate for energy loss due to both wakefields and FEL radiation), followed by another verification of  $K$  values and phase shifter settings. Finally, a random-walk optimization of the electron orbit in the undulator section is performed with the aim of maximizing the photon pulse energy recorded by the photon gas detector.

Figure 5 shows a typical gain curve, obtained after setting up the FEL. The derived gain length is slightly below two meters, in rough agreement with expectations. The achieved photon pulse energies range between 250  $\mu$ J for 2.3 keV photons generated with the nominal  $K$  value of 1.2 and 350  $\mu$ J for 2.0 keV photons produced with a higher  $K$  value of 1.45, also close to expectation.

## OUTLOOK

The planned beam energy increases in the main linac described above, and further tests of all systems at higher repetition rates in the coming months, pave the way to nominal performance of SwissFEL. The schedules for both machine development as well as photonics and experiment commissioning have been tailored to the performance increases.

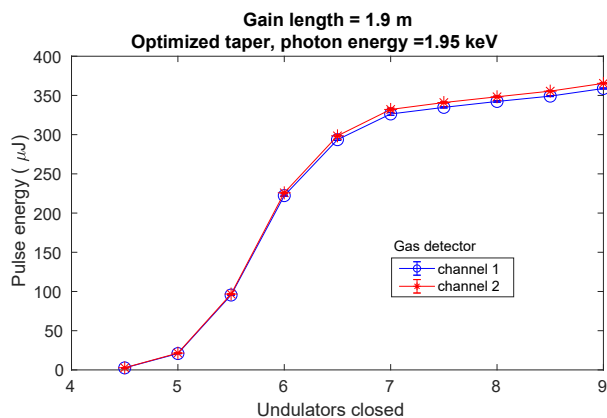


Figure 5: Undulator gain curve measured after FEL setup.

### Aramis Experiment Schedule

SwissFEL Aramis has now completed its first phase of pilot experiments, with two more phases to follow. The second phase will last from June to August of this year and comprises again four pilot experiments, still to be carried out at reduced performance levels with respect to the SwissFEL design values. In the third pilot phase, scheduled to last from October to December, the full performance level should be available (i.e., photons with up to 12.4 keV energy at 100 Hz pulse rate). This last pilot phase will be utilized to consolidate and characterize machine performance before starting the first regular user operation run in early 2019.

The commissioning of optical components, photon diagnostics and the experimental stations will proceed throughout 2018, in parallel with the machine development and consolidation program.

### Athos Soft-X-Ray Line

The extensively redesigned Athos beam line [13] for the generation of soft X-rays in the range 250–1900 eV is currently under construction. Its main features are 16 Apple-X U38 undulators providing full polarization and transverse gradient control, with small magnetic chicanes between them to enable high-performance modes going by names such as “optical klystron,” “high brightness” or “terawatt-attosecond” [14]. In addition, a larger magnetic chicane at the center of the undulator line will allow for two-color operation with controllable delay between the pulses up to 500 fs.

A resonant kicker magnet system [15], custom-designed to divert the two bunches separated by 28 ns into the respective beam lines, was installed earlier this year and has recently undergone first tests with beam. So far only the transport into the Aramis line has been tested—first beam in the Athos dogleg is scheduled for June 2018.

A first undulator prototype is expected to arrive at PSI in June 2018, the installation of the complete undulator line is scheduled for the period from January 2019 to March 2020. The goal is to carry out a first pilot experiment before the end of 2020, with regular user operation to start in 2021.

## CONCLUSION

SwissFEL has reached its 2017 milestone of first pilot experiments at the Aramis hard-X-ray line, albeit with still reduced performance with respect to design parameters (2.3 keV photons at a pulse rate of 10 Hz, as opposed to 12.4 keV at 100 Hz). The current system upgrade and beam development program is on track to reach nominal performance before the end of 2018, such that regular user operation can start in 2019. Meanwhile the installation of the Athos soft-X-ray line is progressing well, aiming at commissioning and first pilot experiments before the end of 2020.

## ACKNOWLEDGMENTS

It is a pleasure to acknowledge the valuable contributions of all the PSI support groups towards the first user operation runs at SwissFEL. Warm thanks go to the experimental teams for the vibrant and enjoyable collaboration during the first pilot experiments. Furthermore we are indebted to Klaus Sokolowski-Tinten for providing Bi film samples.

## REFERENCES

- [1] C. J. Milne *et al.*, *Appl. Sci.*, vol. 7, p. 720, 2017.
- [2] H. H. Braun, “Commissioning of SwissFEL”, presented at IPAC’17, Copenhagen, Denmark, May 2017, WEZA1.
- [3] T. Schietinger *et al.*, *Phys. Rev. Accel. Beams*, vol. 19, p. 100702, 2016.
- [4] F. Loehl, in *Proc. LINAC’16*, East Lansing, MI, USA, Sep. 2016, pp. 22–26.
- [5] M. Aiba and M. Böge, in *Proc. FEL’12*, Nara, Japan, Aug. 2012, pp. 293–296.
- [6] M. Calvi *et al.*, in *Proc. FEL’14*, Basel, Switzerland, Aug. 2014, pp. 107–110.
- [7] B. Keil *et al.*, in *Proc. IBIC’13*, Oxford, UK, Sep. 2013, pp. 427–430.
- [8] F. Frei *et al.*, in *Proc. IBIC’13*, Oxford, UK, Sep. 2013, pp. 769–771.
- [9] V. Arsov *et al.*, to appear in *Proc. IBIC’17*, Grand Rapids, MI, USA, Sep. 2017, doi:10.18429/JACoW-IBIC2017-TUPCC15.
- [10] R. Ischebeck, E. Prat, V. Thominet, and C. Ozkan Loch, *Phys. Rev. ST Accel. Beams*, vol. 18, p. 082802, 2015.
- [11] I. Zagorodnov and M. Dohlus, *Phys. Rev. ST Accel. Beams*, vol. 14, p. 014403, 2011.
- [12] M. Pedrozzi, *et al.*, in *Proc. FEL’14*, Basel, Switzerland, Aug. 2014, pp. 871–877.
- [13] R. Ganter (ed.), SwissFEL Athos conceptual design report, PSI Report No. 17-02, 2017.
- [14] E. Prat, M. Calvi, R. Ganter, S. Reiche, T. Schietinger, and T. Schmidt, *J. Synchrotron Rad.*, vol. 23, pp. 861–868, 2016.
- [15] M. Paraliiev, C. Gough, S. Dordevic, and H. Braun, in *Proc. FEL’14*, Basel, Switzerland, Aug. 2014, pp. 103–106.